Neuron, Vol. 43, 359–372, August 5, 2004, Copyright ©2004 by Cell Press

EMX2 Regulates Sizes and Positioning of the Primary Sensory and Motor Areas in Neocortex by Direct Specification of Cortical Progenitors

Tadashi Hamasaki,[1] Axel Leingärtner,[1] Thomas Ringstedt,[2] and Dennis D.M. O'Leary*
Molecular Neurobiology Laboratory
The Salk Institute
10010 North Torrey Pines Road
La Jolla, California 92037

Summary

Genetic studies of neocortical area patterning are limited, because mice deficient for candidate regulatory genes die before areas emerge and have other complicating issues. To define roles for the homeodomain transcription factor EMX2, we engineered *nestin-Emx2* transgenic mice that overexpress *Emx2* in cortical progenitors coincident with expression of endogenous *Emx2* and survive postnatally. Cortical size, lamination, thalamus, and thalamocortical pathfinding are normal in homozygous *nestin-Emx2* mice. However, primary sensory and motor areas are disproportionately altered in size and shift rostrolaterally. Heterozygous transgenics have similar but smaller changes. Opposite changes are found in heterozygous *Emx2* knockout mice. *Fgf8* expression in the commissural plate of *nestin-Emx2* mice is indistinguishable from wild-type, but *Pax6* expression is downregulated in rostral cortical progenitors, suggesting that EMX2 repression of PAX6 specification of rostral identities contributes to reduced rostral areas. We conclude that EMX2 levels in cortical progenitors disproportionately specify sizes and positions of primary cortical areas.

Introduction

The mammalian neocortex, the largest region of the cerebral cortex, is tangentially organized into subdivisions, called areas, that serve unique functions such as sensory perception or motor control. Areas are also distinguished by distinct architecture, distributions of neuron types, and axon projections. The development of areas is proposed to be controlled by transcription factors (TFs) that specify positional or area identities of cortical neurons and thalamocortical axons (TCAs) that relay visual, auditory, and somatic input to the neocortex (Rakic, 1988; O'Leary, 1989; O'Leary and Nakagawa, 2002). TFs high in the genetic hierarchy controlling arealization should confer positional, or areal, identity to progenitors in the neocortical ventricular zone (VZ) that is imparted to their progeny and also specify the expression of guidance molecules that control area-specific targeting of TCAs. The related homeodomain TFs *Emx1* and *Emx2* are expressed by cortical progenitors in the VZ of dorsal telencephalon (dTel) in a low rostral-lateral to high caudal-medial gradient (Simeone et al., 1992a, 1992b) and are proposed to control arealization (O'Leary et al., 1994). Changes in patterns of gene markers and area-specific TCA projections in embryonic *Emx2* mutant mice provide evidence consistent with a role for EMX2 in arealization (Bishop et al., 2000, 2002; Mallamaci et al., 2000a). In contrast, analyses of *Emx1* mutants and *Emx1/Emx2* double mutants suggest that EMX1 does not regulate arealization (Bishop et al., 2002).

Studies of genetic regulation of areal patterning have been indirect, because mice deficient for *Emx2* or other TFs that are proposed to be primary regulators, for example, PAX6, die perinatally or earlier, before areas emerge. In addition, they have reduced cortical size, which is suggested to be due to region-specific loss of cortical tissue, introducing caveats into interpretations of marker shifts (Muzio et al., 2002b). Further, TCAs either do not reach cortex, as in *Pax6* mutants (Jones et al., 2002), or only a proportion do, as in *Emx2* null mice (Lopez-Bendito et al., 2002), which can alter areal distributions of TCAs (Garel et al., 2002). Thus, evidence for genetic regulation of arealization is controversial.

The goal of this study was to determine whether EMX2 has a primary role in patterning of the neocortex into defined areas. Therefore, we made mice with an *Emx2* transgene driven by promoter elements of the *nestin* gene (*ne*), resulting in its expression being limited to the same progenitors and the same time frame as endogenous *Emx2* in wild-type (wt) cortex. We complement these gain-of-function studies with analyses of heterozygous *Emx2* knockout mice. Our analyses are focused on primary cortical areas because they can be clearly delineated, and markers for higher-order areas are lacking. We also determined the influence of the *Emx2* transgene on expression of the morphogen *Fgf8* in the commissural plate, a domain at the rostral midline of the nascent dTel, because a recent report concluded that EMX2 does not directly control arealization but instead acts solely by repressing *Fgf8* (Fukuchi-Shimogori and Grove, 2003). Our findings lead us to conclude that EMX2 expressed in cortical progenitors disproportionately controls in a direct, concentration-dependent manner the sizes and positioning of primary cortical areas.

Results

ne-Emx2 Transgenic Mice and *Emx2* Transgene Expression

Figure 1A schematizes *Emx2* expression in wt and *ne-Emx2* mice and our findings of overexpressing *Emx2* on patterning of the neocortex into primary areas. *ne-Emx2* transgenic mice were generated using regulatory sequences of the *nestin* gene (*ne*) to drive cDNA of the *Emx2* coding region (Figure 1B) specifically in nestin-positive cells in the nervous system, which are predominantly progenitors in neuroepithelia (Zimmerman et al., 1994). *ne-Emx2* mice are identified by PCR (Figure 1C); transgene expression is detected by qualitative RT-PCR in all brain regions analyzed (Figure 1D and data not shown). Northern blot analysis on forebrain at E11.5 and

*Correspondence: doleary@salk.edu
[1]These authors contributed equally to this work.
[2]Present address: Karolinska Institute, Department of Women and Child Health, Neonatology Unit, Stockholm, Sweden.

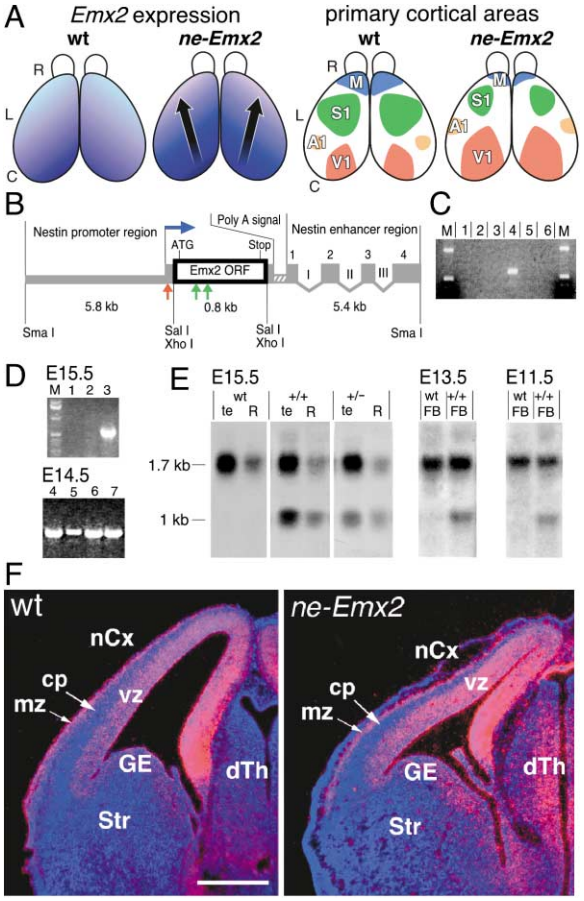

Figure 1. Predicted Effects of *Emx2* Overexpression and Generation of *ne-Emx2* Transgenic Mice

(A) Dorsal views of mouse neocortex. *Emx2* expression: (left) wild-type (wt) mice exhibit a low rostral-lateral to high caudal-medial graded expression; (right) *ne-Emx2* mice have a similar graded expression but at a higher overall level. Arrows indicate the predicted shifts in area identity in *ne-Emx2* mice. Primary cortical areas: (left) organization of adult wt mouse neocortex into primary areas: motor (M), visual (V1), auditory (A1), and somatosensory (S1). (Right) We predict that *Emx2* overexpression in cortical progenitors results in disproportionate increases and reductions in sizes of primary cortical areas and shifts of their positions along the cortical axes. C, caudal; L, lateral; R, rostral.

(B) *ne-Emx2* expression construct (see the Experimental Procedures). The transcription start site of the transgene is indicated by a horizontal arrow; vertical arrows show the locations of primers that were used for PCR genotyping and for RT-PCR mRNA detection.

(C) PCR genotyping *ne-Emx2* mice. Genomic DNA was PCR amplified for the transgene-specific fragment and fractionated by agarose gel electrophoresis. Results from six mice are shown. Line 4 reveals the 0.59 bp transgene-specific PCR product, identifying integration of the transgene. All other lines are wt. M, DNA marker.

(D) Qualitative RT-PCR analysis of *ne-Emx2* transgene expression. RT-PCR was performed with DNase-treated RNA extracted from E15.5 and E14.5 mouse brain. The primer that was used for reverse transcription (RT) was *Emx2* specific, and the nested primers for two subsequent PCR amplifications were *Emx2* specific (antisense primers) and *nestin* specific (sense primer), leading to amplification of a *ne-Emx2* transgene-specific fragment. RT-PCR products were separated by agarose gel electrophoresis. (Lane 1) Control RT-PCR reaction performed with RNA template extracted from wt forebrain; no unspecific amplification product is present. (Lane 2) Control RT-PCR reaction to exclude potential contamination. The reaction was performed with RNA from forebrain of a E14.5 *ne-Emx2* transgenic mouse, but RT was omitted. No band is detected. (Lane 3) RT-PCR reaction with an aliquot of the same RNA that was used in lane 2 (from transgenic embryo) but with RT. A band of 0.59 kb indicates expression of *Emx2* transgene in the transgenic mouse forebrain. (Lanes 4 through 7) RT-PCR with RNA from the following brain regions of an E14.5 *ne-Emx2* transgenic embryo: dTel (lane 4), vTel (lane 5), diencephalon (lane 6), and midbrain (lane 7). All brain regions that were analyzed express the *Emx2* transgene. (Each sample was tested in a control RT-PCR reaction without RT for being free of genomic DNA contamination; data not shown.)

(E) Northern blot analysis of transgene expression. RNA was extracted from telencephalon (te) and the remaining parts of the brain (R) or from forebrain (FB) of E15.5, E13.5, and E11.5 wild-type (wt), *ne Emx2* heterozygous (+/−), and *ne-Emx2* homozygous (+/+) embryos. Blots hybridized with a ^{32}P-labeled *Emx2* cRNA probe reveal in wt and *ne-Emx2* mice a 1.7 kb band that corresponds to endogenous *Emx2* mRNA and a 1 kb band in *ne-Emx2* mice only that corresponds to the *Emx2* transgene mRNA. Relative levels of *Emx2* expression were quantified by densitometry. *Emx2* transgene levels relative to endogenous *Emx2* expression are as follows: homozygous *ne-Emx2* mice, E11.5, 42% ± 2% SEM; E13.5, 39% ± 3%; E15.5, 48% ± 2%; heterozygous *ne-Emx2* mice, E15.5, 26% ± 1%.

(F) *Emx2* expression in wt and *ne-Emx2* mice. In situ hybridization on coronal sections through forebrain of E14.5 wt and *ne-Emx2* mice using ^{35}S-labeled riboprobes for full-length coding region of *Emx2*. Panels are overlays using dark field with a red filter to view silver grains and UV fluorescence to view DAPI counterstain. *Emx2* expression is normally graded high medial/low lateral in the ventricular zone (VZ) of neocortex (nCx) but has limited or no expression elsewhere. In *ne-Emx2* mice, *Emx2* is more highly expressed in the cortical VZ and ganglionic eminence (GE) and is expressed in other proliferative zones that normally do not express *Emx2* but do express nestin, e.g., the VZ of dorsal thalamus (dTh). In wt and *ne-Emx2* mice, *Emx2* expression is seen in Cajal-Retzius neurons of the marginal zone (mz) (Mallamaci et al., 2000b). cp, cortical plate; Str, striatum. Scale bar, 500 μm.

E13.5 and telencephalon at E15.5, ages that encompass most of cortical neurogenesis, reveals in wt and *ne-Emx2* mice a 1.7 kb band corresponding to endogenous *Emx2* mRNA; an additional 1 kb band corresponding to transgene *Emx2* mRNA is observed only in *ne-Emx2* mice (Figure 1E). Densitometry of Northern blots indicates that transgene expression in homozygous *ne-Emx2* mice is about half that of endogenous *Emx2*, and in heterozygous *ne-Emx2* mice the level is about a quarter.

The *ne* vector drives expression across the neocortical VZ in the same progenitors that normally express *Emx2* over a similar period of development (*Emx2*, Simeone et al., 1992a, 1992b; *nestin*, Dahlstrand et al., 1995; *nestin* transgene, Ringstedt et al., 1998; Magdaleno et al., 2002). To localize expression, in situ hybridization was performed on sections through forebrain of wt and *ne-Emx2* mice using an *Emx2* riboprobe at successive days from E10.5 to E15.5 (Figure 1F and data not shown; also Figures 7A and 7B). Figure 1F illustrates expression at E14.5, a peak of cortical neurogenesis, of endogenous *Emx2* in wt and combined expression of endogenous and transgene *Emx2* in *ne-Emx2* mice. In wt, *Emx2* transcripts are distributed in a high caudomedial to low rostrolateral gradient in the cortical VZ, and a low expression is detected in the ganglionic eminence. In *ne-Emx2* mice, a high caudomedial to low rostrolateral gradient of *Emx2* transcripts is evident in the cortical VZ, and expression is higher than that in wt (Figure 1F). Enhanced *Emx2* expression is also evident in the

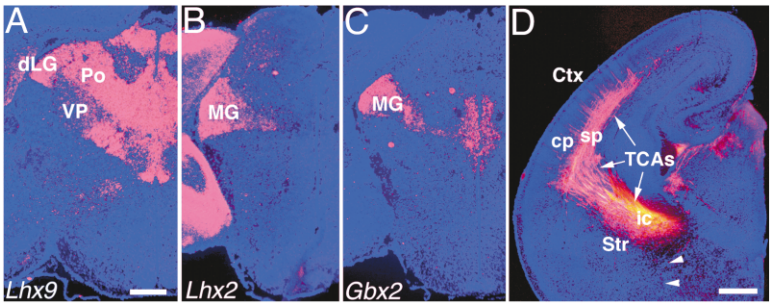

Figure 2. *ne-Emx2* Mice Have Normal Patterning of Dorsal Thalamus and TCA Pathfinding

(A–C) Patterning of dorsal thalamus (dTh) is normal in *ne-Emx2* mice. In situ hybridizations on coronal sections through diencephalon of P0 *ne-Emx2* mice using ^{35}S-labeled riboprobes for (A) *Lhx9*, (B) *Lhx2*, and (C) *Gbx2*. dLG, dorsal lateral geniculate; MG, medial geniculate; VP, ventroposterior; Po, posterior nucleus. These patterns in *ne-Emx2* mice are indistinguishable from wt at P0 and E15 (data not shown) (for wt, see Nakagawa and O'Leary, 2001). Scale bar, 500 μm.

(D) TCA pathfinding is normal in *ne-Emx2* mice. Coronal section through forebrain of an E17 *ne-Emx2* mouse with a large DiI crystal placed in the dTh to label TCAs (arrows). TCA pathfinding in *ne-Emx2* mice is indistinguishable from wt (see Braisted et al., 1999). In *Emx2* null mice, some TCAs exhibit a pathfinding defect and continue along a ventral path (Lopez-Bendito et al., 2002) marked by arrowheads, but this defect is not seen in *ne-Emx2* mice. cp, cortical plate; Ctx, neocortex; ic, internal capsule; sp, subplate; Str, striatum. Scale bar, 500 μm.

ganglionic eminence of *ne-Emx2* mice, and moderate expression is detected in other nestin-positive proliferative zones, such as in dTh, where expression is not detected in wt (Figure 1F).

Thalamic Patterning, TCA Pathfinding, Cortical Size, and Lamination Are Normal in *ne-Emx2* Mice

To address whether potential changes in principal dTh nuclei and TCA input influence cortical patterning, we show using gene markers and histological stains that patterning and size of dTh in *ne-Emx2* mice at E15.5 and P0 (Figures 2A–2C and data not shown) are indistinguishable from wt (see Nakagawa and O'Leary, 2001). DiI axon labeling from dTh confirms that TCA pathfinding is normal in *ne-Emx2* mice (Figure 2D and data not shown; for wt see Braisted et al., 1999). *Emx2* null mice have lamination defects (Mallamaci et al., 2000b), and cortical area is reduced by 30% at P0 (Bishop et al., 2003). However, cortical area, laminar thickness and differentiation, and TCA terminations are normal in *ne-Emx2* mice, at early and late postnatal ages (see Supplemental Figure S1 at http://www.neuron.org/cgi/content/full/43/3/359/DC1).

S1 Is Reduced in Size and Shifts Rostrally and Laterally in *ne-Emx2* Cortex

We predicted that *Emx2* overexpression would result in a reduced size of S1 and a rostral and lateral shift in its location (Figure 1A). To delineate S1, we performed cytochrome oxydase (CO) histochemistry on tangential sections through flattened cortices of P7 wt and *ne-Emx2* mice to reveal the body representation in S1 that parallels its functional organization (Figure 3) (Wong-Riley and Welt, 1980). S1 is significantly reduced in size and shifted rostrally in *ne-Emx2* mice compared to wt (Figure 3A; Table 1). To assess S1 size, we measured the area of the posteromedial barrel subfield (PMBSF), the representation in S1 of large facial whiskers, and related it to the area of the entire neocortex. PMBSF is 25% smaller in *ne-Emx2* mice compared to wt (Figure 3B; Table 1). The CO-negative cortical field rostral to S1, where motor areas are located, is significantly reduced in *ne-Emx2* mice (Figure 3C; Table 1), whereas the cortical field caudal to S1, where visual areas are located, is significantly increased (Figure 3D; Table 1).

To quantify the rostral shift of S1 in *ne-Emx2* mice, we plotted the position of the C3 barrel, located near the center of PMBSF. C3 is positioned more rostrally and laterally in *ne-Emx2* mice than in wt (Figure 3E; Table 1). Distributions of C3 barrel positions in *ne-Emx2* and wt mice do not overlap along the rostral-caudal cortical axis, indicating that the shifts in areal patterning are present in each *ne-Emx2* mouse that was analyzed.

Primary Sensory Areas Show Disproportionate Changes in Sizes and Position Shifts in *ne-Emx2* Cortex

To analyze the effect of *Emx2* overexpression on each primary sensory area, we used serotonin immunostaining on tangential sections through flattened cortices of P7 wt and *ne-Emx2* mice to mark TCA terminations of the ventroposterior nucleus (VP), dorsal lateral geniculate nucleus (dLG), and ventral division of the medial geniculate nucleus (MGv) in layer 4 (Fujimiya et al., 1986), revealing the size and position of the primary sensory areas to which they project, the primary somatosensory area (S1), primary visual area (V1), and primary auditory area (A1), respectively (Figure 4A). V1 is significantly larger in homozygous *ne-Emx2* mice compared to wt (Figures 4A–4C): V1 length is 38% greater than in wt (Figure 4D), and its area is increased 52% relative to overall cortical area (Figure 4E). The rostral border of V1 shifts rostrally, whereas its caudal border remains fixed near the caudal flexure of the hemisphere. A1 is also significantly shifted rostrally and laterally in homozygous *ne-Emx2* mice compared to wt (Figure 4F). Positions of A1 in the two populations do not overlap along either cortical axis. These data show that the primary sensory areas exhibit disproportionate changes in their sizes in *ne-Emx2* mice compared to wt, with S1 decreasing and V1 increasing, and the primary sensory areas, including A1, shift rostrally and laterally (Table 1).

Disproportionate Changes in Motor and Visual *cad8* Domains in *ne-Emx2* Cortex

To address whether cortical plate neurons exhibit changes in positional, or areal, identities, we analyzed the expression pattern of *cadherin8* (*cad8*), a cell adhesion protein expressed by cortical plate neurons in patterns that mark V1 and the motor area in postnatal mice (Suzuki et al., 1997). Because the *cad8* expression do-

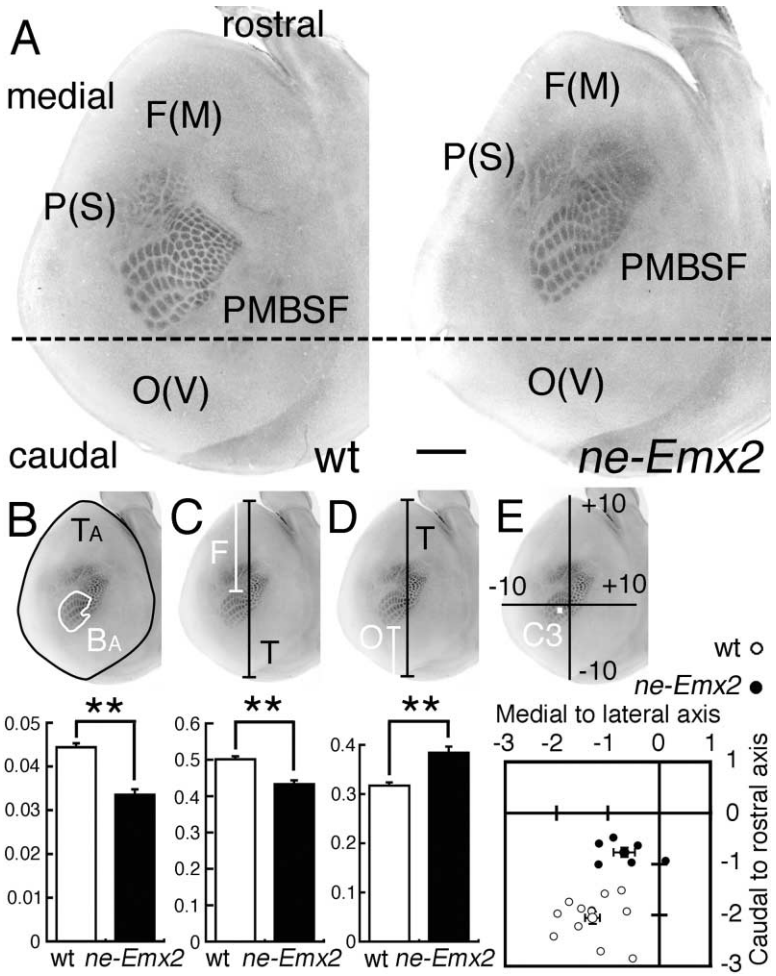

Figure 3. Reduced Size and Rostrolateral Shift of S1 in *ne-Emx2* Mice

(A) CO histochemistry on tangential sections of flattened cortices of P7 wild-type (wt) and *ne-Emx2* mice. CO is a mitochondrial enzyme enriched in TCA terminations and presynaptic dendrites in layer 4, and by P7, CO staining reveals S1 that includes the barrel pattern of facial whiskers in posteromedial barrel subfield (PMBSF). In *ne-Emx2* mice, S1 is reduced in size and shifted rostrally compared to wt (dashed line is at the same rostral-caudal level in both). F(M), frontal cortex (motor areas); O(V), occipital (visual areas); P(S), parietal (somatosensory areas). Scale bar, 1 mm.

(B) PMBSF ratio, defined as the ratio of B_A (the area of PMBSF) to T_A (the area of the entire cortex).

(C) Frontal ratio, defined as the ratio of F (the length from the frontal pole to the rostral edge of PMBSF) to T (the length from the frontal pole to the occipital pole).

(D) Occipital ratio, defined as the ratio of O (the length from the occipital pole to the caudal edge of the PMBSF) to T.

(E) Scatter plot of C3 barrel position, located near the center of PMBSF. Coordinate axes were drawn on sections as shown: the caudal-rostral (C-R) axis extends from the occipital pole to the frontal pole, and the medial-lateral (M-L) axis is at the widest aspect of the section. In *ne-Emx2* mice (black dots), C3 is rostral and lateral to C3 in wt (open circles). The difference between the C-R and M-L location of C3 in wt and *ne-Emx2* is significant (C-R, $p < 0.001$; M-L, $p < 0.05$). In (B)–(D), ** indicates significance of $p < 0.01$ in unpaired Student's t test. See Table 1 for summary.

mains develop independent of TCA input (Nakagawa et al., 1999) and expand or contract in *Emx2* and *Pax6* mutants, respectively, as predicted, *cad8* is considered a bona fide positional marker in neocortex (Bishop et al., 2000, 2002).

We performed whole-mount in situ hybridizations for *cad8* on P7 brains (Figure 5A) and measured the sizes of the motor and V1 *cad8* domains (Figure 5B). The motor *cad8* domain is 36% smaller in *ne-Emx2* mice compared to wt (Figure 5B; Table 1), whereas the V1 *cad8* domain is 24% larger (Figure 5C; Table 1). These findings show that *Emx2* overexpression in cortical progenitors changes the positional identities of their progeny, including cortical plate neurons. These disproportionate changes in *cad8* domains in *ne-Emx2* mice are consistent with our CO (Figure 3) and serotonin (Figure 4) analyses that show that the frontal (motor) cortical field rostral to S1 is decreased in *ne-Emx2* mice and that the occipital (visual) cortical field caudal to S1, as well as V1 itself, are increased (Table 1).

Caudal Areas Exhibit Enhanced Sensitivity to *Emx2* Overexpression

P7 heterozygous *ne-Emx2* mice have a subset of phenotypes described above for homozygous *ne-Emx2* mice. Analyses of CO- and serotonin-stained tangential sections from P7 flattened cortices do not reveal significant differences in S1 size or shifts in its location in heterozygous *ne-Emx2* mice (data not shown). However, analyses using serotonin immunostaining show that V1 in P7 heterozygous *ne-Emx2* mice (Figure 4B) is intermediate in size to V1 in wt (Figure 4A) and homozygous *ne-Emx2* mice (Figure 4C) and significantly different from either (Figures 4D and 4E; Table 1). In heterozygous *ne-Emx2* mice, V1 length is 16% greater than in wt (Figure 4D), and V1 area is increased 25% (Figure 4E). In addition, A1 is significantly shifted rostrally and laterally in heterozygous *ne-Emx2* mice (Figures 4B and 4F) compared to wt (Figures 4A and 4F) (Table 1). These findings indicate that caudal neocortex is particularly sensitive to *Emx2* overexpression and support the suggestion that EMX2 preferentially imparts caudal area identities.

Fgf8 Expression in the Commissural Plate Is Normal in *ne-Emx2* Mice

Emx2 expression in dTel begins at E8.5 (Simeone et al., 1992a, 1992b), similar to *Fgf8* expression in the commissural plate (Shimamura and Rubenstein, 1997). Fukuchi-Shimogori and Grove (2003) report that ectopic *Emx2* expression in the *Fgf8* domain in the commissural plate that is achieved by electroporation results in a dramatic downregulation of *Fgf8* and a substantial reduction in

Table 1. Summary of Statistical Analyses of Neocortical Areas in *ne-Emx2* Transgenic Mice

					ne-Emx2 Mice					
Neocortical Area	Parameter	Marker/Experiment	wt ± SEM	n	hetero ± SEM	inc/dec/sh	n	homo ± SEM	inc/dec/sh	n
Motor area	frontal length (mm)	CO, flat cortex	3.94 ± 0.10	14				3.38 ± 0.14**	14% dec	6
(frontal cortex)	frontal area (mm^2)	cad8, WMISH	3.34 ± 0.11	16				1.98 ± 0.13***	41% dec	8
	frontal length ratio	CO, flat cortex	0.501 ± 0.009	14				0.433 ± 0.006***	14% dec	6
	frontal area ratio	cad8, WMISH	0.170 ± 0.003	16				0.109 ± 0.002***	36% dec	8
Somatosensory area	PMBSF area (mm^2)	CO, flat cortex	1.58 ± 0.03	14				1.17 ± 0.09**	26% dec	6
(parietal cortex)	PMBSF area ratio	CO, flat cortex	0.044 ± 0.001	14				0.034 ± 0.002**	25% dec	6
	C3 C-R location	CO, flat cortex	−2.05 ± 0.12	12				−0.77 ± 0.09***	6% R/sh	6
	C3 M-L location	CO, flat cortex	−1.30 ± 0.15	12				−0.68 ± 0.21*	3% L/sh	6
Auditory area	A1 C-R location	5HT, flat cortex	−5.27 ± 0.19	10	−4.31 ± 0.12††	5% R/sh	7	−3.52 ± 0.13†††	9% R/sh	8
(temporal cortex)	A1 M-L location	5HT, flat cortex	1.83 ± 0.19	10	3.12 ± 0.19†††	6% L/sh	7	3.97 ± 0.15†††	11% L/sh	8
Visual area	occipital length (mm)	CO, flat cortex	2.49 ± 0.07	14				2.99 ± 0.12**	20% inc	6
(occipital cortex)	occipital area (mm^2)	cad8, WMISH	3.21 ± 0.06	16				3.75 ± 0.14**	17% inc	7
	V1 length (mm)	5HT, flat cortex	1.92 ± 0.05	15				2.65 ± 0.16***	38% inc	4
	V1 area (mm^2)	5HT, flat cortex	2.19 ± 0.07	15				3.00 ± 0.23***	37% inc	4
	occipital length ratio	CO, flat cortex	0.317 ± 0.007	14				0.384 ± 0.010***	21% inc	6
	occipital area ratio	cad8, WMISH	0.165 ± 0.004	16				0.205 ± 0.005***	24% inc	7
	V1 length ratio	5HT, flat cortex	0.235 ± 0.008	15	0.272 ± 0.005†	16% inc	7	0.323 ± 0.008†††	38% inc	10
	V1 area ratio	5HT, flat cortex	0.059 ± 0.002	15	0.073 ± 0.001††	25% inc	7	0.089 ± 0.003†††	52% inc	10

Table presents mean data and standard error of the mean (SEM) for the number of cases (n) indicated. For each neocortical area data set, the first set of data are absolute measurements, whereas the second set of data (indicated as "ratio") are proportional relative to overall area or length. Proportional data are presented in the text. Some cases were only suitable for one or the other type of measurements. wt, wild type; inc/dec, increase or decrease rate compared to wild type; CO, cytochrome oxydase; cad8, cadherin8; WMISH, whole-mount in situ hybridization; PMBSF, posteromedial barrel subfield; C3, barrel C3; C-R, caudal to rostral; R/sh, shift toward rostral pole in percent of caudal to rostral cortical axis; M-L, medial to lateral; L/sh, shift toward lateral margin in percent of medial to lateral cortical axis; A1, primary auditory area; 5HT, 5-hydroxytryptamine (serotonin); V1, primary visual area. *$p < 0.05$; **$p < 0.01$; ***$p < 0.001$, compared to wt by unpaired Student's t test. †$p < 0.05$; ††$p < 0.01$; †††$p < 0.001$, compared to wt by ANOVA/Bonferroni's multiple comparison.

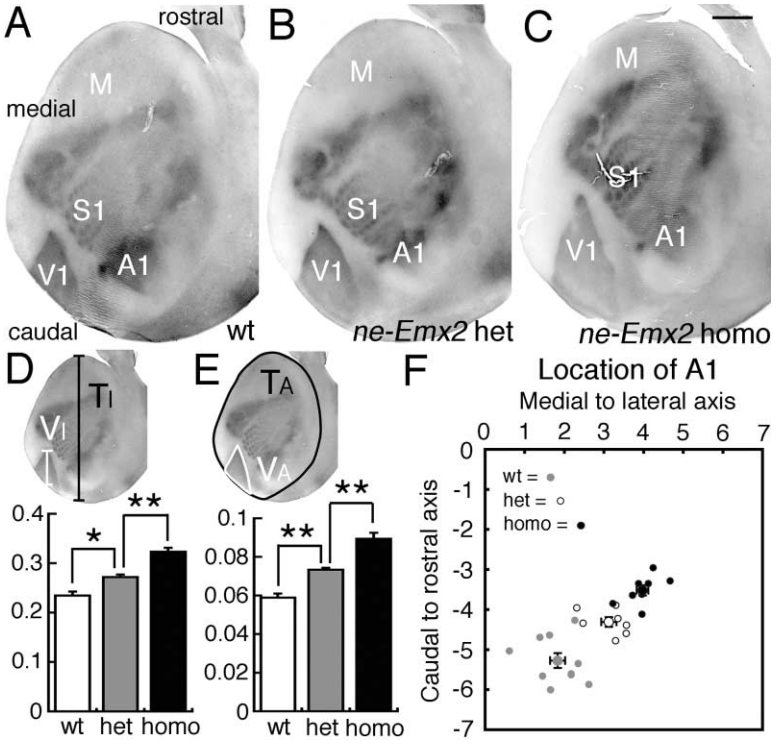

Figure 4. Disproportionate Changes in Sizes of Primary Sensory Areas and Shifts in Their Locations in an *Emx2* Concentration-Dependent Manner in *ne-Emx2* Mice

(A–C) Serotonin immunostaining on tangential sections of flattened cortex of P7 wild-type (wt; [A]), heterozygous *ne-Emx2* (het; [B]), and homozygous *ne-Emx2* (homo; [C]) mice. In *ne-Emx2* homo (C), V1 expands compared to wt, S1 is reduced in size and shifts rostrally, A1 shifts rostrolaterally, and the domain remaining for motor areas (M) is reduced compared to wt. In *ne-Emx2* het (B), these changes are intermediate. Scale bar in (C) is 1 mm for (A)–(C).

(D) Histogram for V1 length ratio, defined as ratio of V1 length (V_l) relative to the overall cortical length (T_l).

(E) Histogram for V1 area ratio, defined as ratio of V1 area (V_A) relative to the overall cortical area (T_A).

(F) Scatter plot for position of A1. The center of A1 was plotted in coordinate axes similar to the C3 barrel in Figure 3E. The difference of the C-R and M-L locations of A1 between wt, *ne-Emx2* het, and *ne-Emx2* homo is statistically significant. In (D) and (E), * indicates a significance of $p < 0.05$, and ** indicates a significance of $p < 0.01$. See Table 1 for summary.

its expression domain and at later ages in a rostral shift of S1. They conclude that EMX2 does not directly control arealization but acts solely by repressing *Fgf8* expression in the commissural plate. Therefore, we examined in wt and *ne-Emx2* mice the relationships between expression of *Fgf8*, nestin, and *Emx2* in transverse forebrain sections on consecutive days from E9.5 to E12.5 and *Fgf8* expression in the commissural plate in whole mounts at E9.5 and E10.5 (Figure 6).

At E9.5, a low to moderate level of nestin immunostaining is observed throughout most of the telencephalic wall, but a much lower level of nestin staining is observed in the *Fgf8* domain in the commissural plate (Figures 6A–6C′). By E10.5, nestin staining is stronger in the telencephalon and includes the *Fgf8* domain (Figures 6D–6F). This overlap in nestin immunostaining and the *Fgf8* domain persists at E11.5 (data not shown) and E12.5 (Figures 6G–6I). In wt mice of these ages, *Emx2* expression is not detected in the *Fgf8* domain, although we find strong *Emx2* expression dorsal to it (data not shown).

In contrast, in *ne-Emx2* mice, the relationship of *Emx2* expression to the *Fgf8* domain in the commissural plate parallels that of nestin immunostaining, since nestin promoter elements drive expression of the *Emx2* transgene. As a result, in *ne-Emx2* mice at E9.5, *Emx2* expression is very low or nondetectable in the midline *Fgf8* domain, but moderate levels of *Emx2* expression are observed in it at E10.5 (data not shown) and E12.5 in *ne-Emx2* mice (Figures 6J–6L). In *ne-Emx2* mice at E9.5 through E12.5, much stronger *Emx2* expression is seen in the cortical VZ dorsal to the *Fgf8* domain (Figures 6J–6L and data not shown), due to the combined expression of endogenous and transgene *Emx2*.

The *Fgf8* expression domain in the commissural plate has the same appearance, both in size and level of expression, in transverse sections through the telencephalon in wt and *ne-Emx2* mice at E10.5 (data not shown) and E12.5 (Figures 6H, 6I, 6K, and 6L) and in

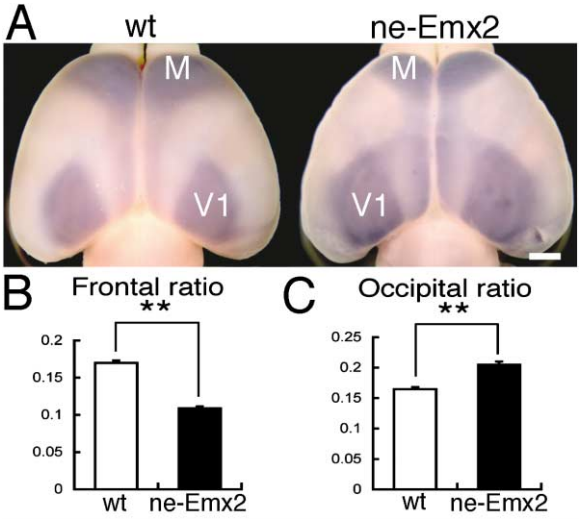

Figure 5. Disproportionate Changes in Size of Motor Area and V1 Domains of *cad8* Expression in *ne-Emx2* Mice

(A) In situ hybridization for *cad8* using digoxigenin-labeled riboprobes on whole mounts of P7 wild-type (wt) and *ne-Emx2* brains to mark the motor area (M) and V1. *ne-Emx2* brain has smaller M and larger V1 *cad8* expression domains. Scale bar, 1 mm.

(B and C) Histograms for ratio of the area of M *cad8* domain (B) and V1 *cad8* domain (C) relative to the dorsal neocortical surface area. ** indicates significance of $p < 0.01$. See Table 1 for summary.

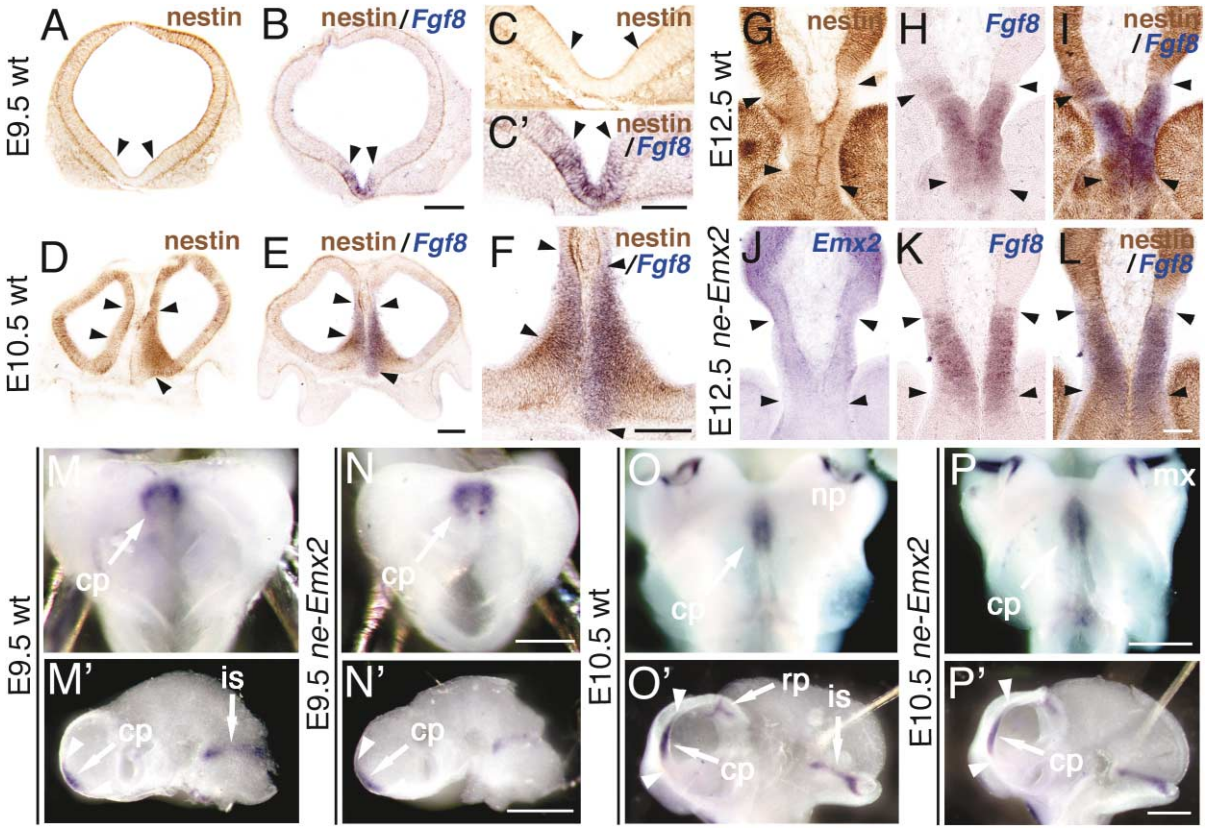

Figure 6. *Fgf8* Expression in the Commissural Plate of *ne-Emx2* Mice Is Indistinguishable from Wild-Type

(A–C′) Coronal sections through the midline *Fgf8* expression domain in commissural plate (cp) of dTel in E9.5 wt. (A and C) Nestin immunostaining. (B and C′) Nestin immunostaining (brown) and *Fgf8* in situ hybridization (blue). High-power views of *Fgf8* domain (between arrowheads in [A] and [B]) are shown in (C) and (C′), respectively. Scale bar in (B) is 200 μm for (A) and (B). Scale bar in (C′) is 100 μm for (C) and (C′). E9.5 analyzed, n = 7.

(D–F) Coronal sections through *Fgf8* domain in the cp of E10.5 wt. (D) Nestin immunostaining. (E and F) Nestin immunostaining (brown) with *Fgf8* in situ hybridization (blue). High-power view of *Fgf8* domain (between arrowheads in [E]) is shown in (F). Scale bar in (E) is 200 μm for (D) and (E). Scale bar in (F) is 200 μm. E10.5 analyzed, n = 5; E11.5 analyzed, n = 2 (data not shown).

(G–I) Adjacent coronal sections through *Fgf8* domain in the cp of E12.5 wt. Nestin immunostaining (G), *Fgf8* in situ hybridization (H), and nestin immunostaining (brown) with *Fgf8* in situ hybridization (blue) (arrowheads mark same points in [G]–[I]). E12.5 analyzed, n = 7.

(J–L) Adjacent coronal sections through *Fgf8* domain in the cp of E12.5 *ne-Emx2* mice. *Emx2* in situ (J), *Fgf8* in situ (K), and nestin immunostaining (brown) with *Fgf8* in situ (blue) (L) (arrowheads mark same points in [J]–[L]). Scale bar in (L) is 100 μm for (G)–(L). *ne-Emx2* mice analyzed: E9.5, n = 2; E10.5, n = 1; E12.5, n = 2.

(M and N) Dorsal view of embryo heads of E9.5 wt (M) and *ne-Emx2* homozygous (N) mice. Arrows indicate the *Fgf8* domain in the cp at the anterior dTel midline. Anterior is to the top. Scale bar in (N) is 250 μm for (M) and (N). (M′ and N′) Midline views of E9.5 wt (M′) and *ne-Emx2* homozygous (N′) brains bisected at the sagittal midline. Arrowheads mark the *Fgf8* expression domain in the cp. Anterior is to the left; dorsal is to the top. The lengths of the *Fgf8* domain in the cp in wt (n = 5 hemispheres, 3 brains) and *ne-Emx2* homozygous (n = 6 hemispheres, 3 brains) are 279.2 ± 4.6 SEM and 274.6 ± 6.3 μm, respectively; the difference is not significant ($p = 0.285$; unpaired Student's t test). is, isthmus. Scale bar in (N′) is 500 μm for (M′) and (N′).

(O and P) Dorsal views of embryo heads of E10.5 wt (O) and *ne-Emx2* homozygous (P). np, nasal pit; mx, maxillary component of the first pharyngeal arch. Scale bar in (P) is 500 μm for (O) and (P). (O′ and P′) Midline views of E10.5 wt (O′) and *ne-Emx2* homozygous (P′) brains. The lengths of the *Fgf8* domain in the cp in wt (n = 4 hemispheres, 2 brains) and *ne-Emx2* homo (n = 6 hemispheres, 3 brains) are 541.0 ± 4.8 and 529.9 ± 9.0 μm, respectively; the difference is not significant ($p = 0.155$; unpaired Student's t test). rp, roof plate. Scale bar in (P′) is 500 μm for (O′) and (P′).

brain whole mounts at E9.5 (Figures 6M–6N′) and E10.5 (Figures 6O–6P′). Measurements of the *Fgf8* domain show that its size is not significantly different between stage-matched wt and *ne-Emx2* mice at E9.5 and E10.5 (Figure 6 legend). Our findings show that expression of *Fgf8* in the commissural plate in *ne-Emx2* mice is indistinguishable from wt at the ages that this *Fgf8* domain influences cortical patterning. Therefore, we conclude that the disproportionate changes in area sizes and positions in *ne-Emx2* mice are not due to repression of *Fgf8* expression by the *Emx2* transgene but instead are due to the direct action of endogenous and transgene *Emx2* in progenitors in the cortical VZ.

Expression of Candidate Arealization Genes in *ne-Emx2* Cortex

PAX6 (Bishop et al., 2000, 2002) and COUP-TF1 (Zhou et al., 2001) are implicated in cortical patterning, and

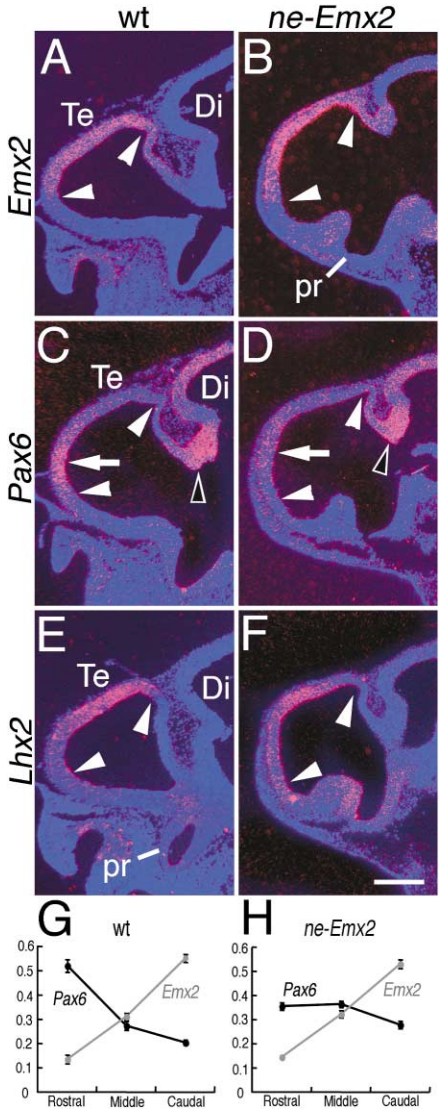

Figure 7. Increased Expression of *Emx2* in *ne-Emx2* Mice Represses *Pax6* Expression

(A–F) In situ hybridizations using ^{35}S-labeled riboprobes for *Emx2*, *Pax6*, and *Lhx2* on sagittal sections through forebrain of E10.5 wild-type (wt) and *ne-Emx2* mice. (A and B) In wt (A), *Emx2* expression is largely limited to dorsal telencephalon (dTel) (arrowheads in [A]). In *ne-Emx2* mice (B), *Emx2* expression is elevated in dTel but retains a high caudal to low rostral gradient as in wt. (C and D) In wt (C), *Pax6* expression extends from dTel into the diencephalon. In *ne-Emx2* mice (D), *Pax6* expression is similar to wt except that the high rostral to low caudal expression that is evident in dTel of wt (C) is flattened due to decreased *Pax6* expression in rostral dTel (marked by arrow in [C] and [D]). Open arrowhead in (C) and (D) marks a strong *Pax6* expression domain in diencephalon. (E and F) In wt (E), *Lhx2* expression in dTel is graded, high caudal to low rostral (arrowheads in [E]). *Lhx2* expression in dTel of *ne-Emx2* mice (F) is similar to wt. Scale bar in (F) is 50 μm for (A)–(F). Di, diencephalon; pr, preoptic recess; Te, dorsal telencephalon.

(G and H) Quantification of expression pattern of *Emx2* and *Pax6* in wt and *ne-Emx2* mice. Graphs show mean silver grain ratios (with standard error bars) at three positions in the VZ of sagittal sections through dTel (as in [A]–[D]) in wt (G) and *ne-Emx2* mice (H). Each data point is the mean of four cases (see the Experimental Procedures).

LHX2 is hypothesized to influence it (Nakagawa et al., 1999; Monuki et al., 2001). Therefore, we examined their expression using in situ hybridization with ^{35}S-labeled riboprobes on sagittal sections of wt and *ne-Emx2* brains at E10.5 (Figure 7), when the first neocortical neurons are generated, and at E12.5 and E15.5 (data not shown). In wt and *ne-Emx2* mice, *Emx2* has a high caudal to low rostral graded expression in the cortical VZ (Figures 7A and 7B). In contrast, the low caudal to high rostral graded expression of *Pax6* in the cortical VZ of wt (Figure 7C) is flattened in *ne-Emx2* mice, due to diminished expression rostrally, where *Pax6* expression is normally strongest (Figure 7D; data not shown). We detect no difference in expression of *Lhx2* (Figures 7E and 7F) or *COUP-TF1* (data not shown) in *ne-Emx2* cortex.

To quantify relative gradients of *Pax6* and *Emx2* expression in the VZ of wt and *ne-Emx2* neocortex, we counted silver grains at equivalent positions along the rostral-caudal axis of sagittal sections through E10.5 neocortex. A robust high rostral to low caudal gradient of *Pax6* and an opposing high caudal to low rostral gradient of *Emx2* are evident in wt (Figure 7G). In *ne-Emx2* mice, *Emx2* retains a robust high caudal to low rostral graded expression, whereas the slope of *Pax6* expression is flattened (Figure 7H). This apparent repression of *Pax6* by *Emx2* overexpression in *ne-Emx2* mice could contribute to the reduced sizes and rostral shifts of rostral areas, such as motor and S1.

Heterozygous *Emx2* Knockout Mice Have Opposite Changes in Primary Areas to Those in *ne-Emx2* Mice

To test whether a decrease in *Emx2* expression influences primary cortical areas in an opposing manner to increasing *Emx2* levels (Figure 8A), we performed on heterozygous *Emx2*$^{+/-}$ knockout mice and wt littermates analyses similar to those that were performed on *ne-Emx2* mice. Northern blot analysis of telencephalon at E12.5, E13.5, and E15.5 reveals in wt and *Emx2*$^{+/-}$ mice a 1.7 kb band that corresponds to endogenous *Emx2* mRNA; densitometry indicates that *Emx2* expression is diminished by a third in *Emx2*$^{+/-}$ mice compared to wt (Figure 8B).

Analyses of CO- and serotonin-stained tangential sections through P7 flattened cortices of wt (*Emx2*$^{+/+}$) (Figure 8C) and *Emx2*$^{+/-}$ littermates (Figure 8D) reveal opposite changes in arealization in *Emx2*$^{+/-}$ than those observed in *ne-Emx2* mice. Overall cortical area in wt and *Emx2*$^{+/-}$ mice is not significantly different (Figure 8E). However, V1 is significantly reduced in size in *Emx2*$^{+/-}$ mice compared to wt: V1 length is 25% less than in wt (Figure 8F; Table 2), and V1 area is reduced by 23% (Figure 8G; Table 2). Consistent with these changes, the rostral-caudal length of occipital cortex compared to overall cortical length is significantly decreased in *Emx2*$^{+/-}$ mice by 13% (Figure 8H; Table 2). In contrast, frontal cortex rostral to S1, where motor areas are located, is significantly increased by 8% in length in *Emx2*$^{+/-}$ mice (Figure 8I; Table 2). PMBSF is 12% larger, and the C3 barrel is positioned more caudally and medially in *Emx2*$^{+/-}$ mice than in wt, but these changes do not achieve statistical significance (Figure 8J; Table 2).

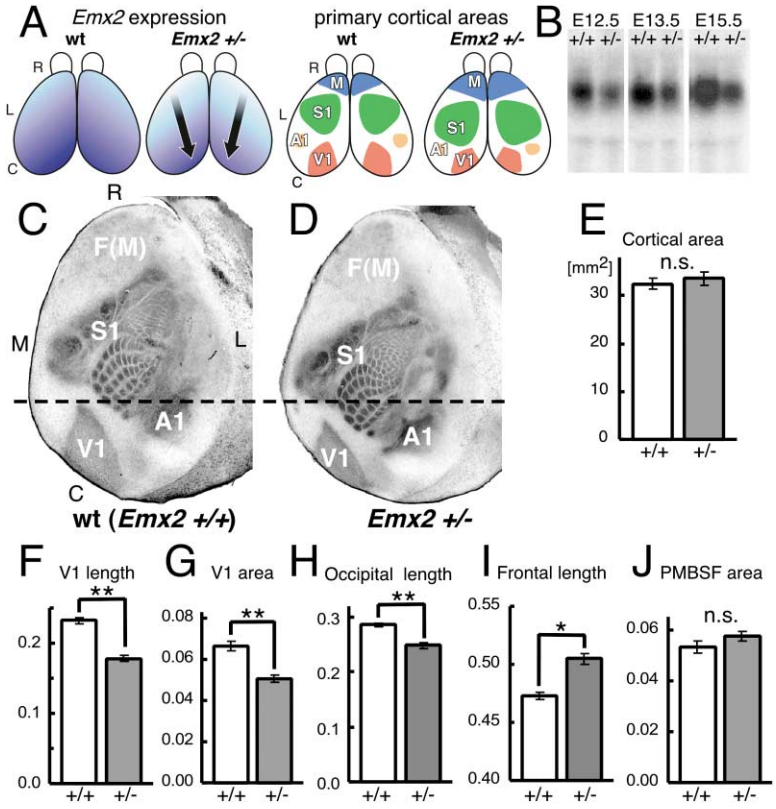

Figure 8. Disproportionate Changes in Sizes of Primary Areas and Shifts in Their Relative Locations in Heterozygous *Emx2* Knockout Mice

(A) Dorsal views of mouse neocortex. *Emx2* expression: (left) wild-type mice (wt) exhibit a low rostral-lateral to high caudal-medial graded expression; (right) a similar graded expression is observed in heterozygous $Emx2^{+/-}$ mice but at a lower overall level. Arrows indicate the predicted and observed shifts in areal patterning in $Emx2^{+/-}$ mice. Primary cortical areas: (left) organization of adult wt ($Emx2^{+/+}$) mouse neocortex into primary areas motor (M), V1, A1, and S1. (Right) We predict and find that $Emx2^{+/-}$ mice have disproportionate increases and decreases in sizes of primary cortical areas and shifts in positions, as schematized. C, caudal; L, lateral; R, rostral.

(B) Northern blot analysis of *Emx2* expression in wt (+/+) and $Emx2^{+/-}$ mice using RNA extracted from telencephalon of E12.5, E13.5, and E15.5 embryos. Hybridization with a ^{32}P-labeled *Emx2* cRNA probe reveals a 1.7 kb *Emx2* mRNA-specific band. Densitometry (see the Experimental Procedures) indicates a similar decrease of *Emx2* mRNA expression in $Emx2^{+/-}$ mice at the three ages that were analyzed (n = 3), with a mean decrease of 34% ± 1% SEM relative to wt littermates (+/+) (n = 3).

(C and D) Serotonin immunostaining on tangential sections of flattened cortex of P7 wt (C) and $Emx2^{+/-}$ (D) mice. The dashed line marks the most rostral edge of V1 in wt (C) and is at the same rostral-caudal position in both genotypes. In $Emx2^{+/-}$ mice (D), V1 is reduced in size, S1 shifts caudally and is slightly increased in size, and the domain remaining for motor areas (M) is increased, compared to wt.

(E) Overall area of flattened cortex of wt and $Emx2^{+/-}$ mice at P7 is not significantly different (n.s.): wt (+/+), 31.3 ± 1.1 mm^2 (n = 8); $Emx2^{+/-}$, 33.6 ± 1.4 mm^2 (n = 7).

(F–J) Histograms of relative length and size of cortical areas and fields from wt ($Emx2^{+/+}$) and $Emx2^{+/-}$ littermates, measured as described in Figures 4D and 4E and Figures 3B–3D. In (F)–(I), * indicates significance of $p < 0.05$, and ** indicates a significance of $p < 0.01$. In (J), PMBSF ratio is increased in $Emx2^{+/-}$ mice compared to wt, but the difference does not reach statistical significance (n.s.). See Table 2 for summary.

These findings show that V1 is reduced in size in $Emx2^{+/-}$ mice compared to wt and that S1 and motor areas are increased in size and shifted caudally. Thus, decreasing *Emx2* expression in cortical progenitors has the opposite effect on areal patterning of the neocortex as increasing *Emx2* expression.

Discussion

EMX2 Levels in Cortical Progenitors Disproportionately Control Sizes and Positioning of Primary Cortical Areas

Emx2 is expressed highest in progenitors that generate caudal-medial areas of neocortex, such as V1, and lowest in progenitors that generate rostral and lateral areas, such as S1 and motor (Simeone et al., 1992a, 1992b; Leingartner et al., 2003). If EMX2 controls arealization, it should preferentially impart caudal-medial area identities. Recent studies present evidence consistent with this hypothesis (Bishop et al., 2000, 2002; Mallamaci et al., 2000a; Leingartner et al., 2003; Muzio and Mallamaci, 2003). However, the findings are controversial, and reinterpretation has been suggested because of defects in TCA pathfinding (Lopez-Bendito et al., 2002) and a potential region-specific loss of cortical tissue (Muzio et al., 2002b) in *Emx2* null mice, and a report concluding that EMX2 acts indirectly in arealization by repressing *Fgf8* expression in the commissural plate (Fukuchi-Shimogori and Grove, 2003).

The present study does not suffer from these caveats, because cortical size and TCA pathfinding are normal in *ne-Emx2* mice and $Emx2^{+/-}$ mice, and *Fgf8* expression in *ne-Emx2* mice is indistinguishable from wt. We show that in *ne-Emx2* mice the primary sensory and motor cortical areas have disproportionate changes in their sizes and shifts in position compared to wt (Figure 1A). V1, a caudomedial area, is significantly increased in size, whereas rostral areas S1 and motor are significantly reduced in size, and all three areas shift rostrally; S1 and A1 shift laterally as well as rostrally. We also find significant changes in the size and positioning of V1 and A1 in heterozygous *ne-Emx2* mice intermediate to wt and homozygous *ne-Emx2* mice, whereas rostral areas S1 and motor do not exhibit significant changes in heterozygous *ne-Emx2* mice.

Complementing the gain-of-function studies in *ne-Emx2* mice, we show that in $Emx2^{+/-}$ mice, which have reduced *Emx2* expression, V1 is significantly reduced in size, and its rostral border is shifted caudally. S1 and the rostral cortical field that contains motor areas are

Table 2. Summary of Statistical Analyses of Neocortical Areas in Heterozygous *Emx2* Knockout Mice

Neocortical Areas	Parameter	Marker/Experiment	*Emx2*$^{+/+}$ ± SEM	n	*Emx2*$^{+/-}$ ± SEM	inc/dec/sh	n
Motor area	frontal length (mm)	CO and 5HT, flat cortex	3.649 ± 0.0842	8	4.061 ± 0.0568	9% inc	8
(frontal cortex)	frontal length ratio	CO and 5HT, flat cortex	0.470 ± 0.0026	10	0.507* ± 0.0038	8% inc	8
Somatosensory area	PMBSF area (mm^2)	CO and 5HT, flat cortex	1.719 ± 0.0536	8	1.954 ± 0.0406	14% inc	8
(parietal cortex)	PMBSF area ratio	CO and 5HT, flat cortex	0.052 ± 0.0022	8	0.058 ± 0.0018	12% inc	8
	C3 C-R location	CO and 5HT, flat cortex	−2.060 ± 0.0442	8	−2.442 ± 0.0958	2% C/sh	8
	C3 M-L location	CO and 5HT, flat cortex	−1.760 ± 0.1092	8	−2.340* ± 0.1256	3% M/sh	8
Visual area	occipital length (mm)	CO and 5HT, flat cortex	2.199 ± 0.0803	9	1.960* ± 0.0539	11% dec	8
(occipital cortex)	V1 length (mm)	5HT, flat cortex	1.755 ± 0.0631	10	1.378** ± 0.0475	21% dec	6
	V1 area (mm^2)	5HT, flat cortex	2.085 ± 0.1134	10	1.711* ± 0.1219	18% dec	6
	occipital length ratio	CO and 5HT, flat cortex	0.286 ± 0.0065	9	0.249** ± 0.0037	13% dec	8
	V1 length ratio	5HT, flat cortex	0.232 ± 0.0037	10	0.174** ± 0.0044	25% dec	6
	V1 area ratio	5HT, flat cortex	0.065 ± 0.0018	10	0.051** ± 0.0015	23% dec	6

Table presents mean data and standard error of the mean (SEM) for the number of cases (n) indicated. For each neocortical area data set, the first set of data are absolute measurements, whereas the second set of data (indicated as "ratio") are proportional relative to overall area or length. Proportional data are presented in the text. Some cases were only suitable for one or the other type of measurements. C-R, caudal to rostral axis; M-L, medial to lateral axis; inc/dec, increase/decrease relative to wild type; C/sh, shift toward caudal pole in percent of caudal to rostral cortical axis; M/sh, shift toward medial margin in percent of medial to lateral cortical axis; C3, barrel C3; PMBSF, posteromedial barrel subfield; CO, cytochrome oxidase; 5HT, 5-hydroxytryptamine (serotonin); V1, primary visual area. *$p < 0.05$; **$p < 0.01$, compared to wt by unpaired Student's t test.

modestly increased in size and shifted caudally, and S1 is shifted medially, but only the effects on motor area size and S1 position are significant. We conclude that EMX2 operates by a concentration-dependent mechanism in cortical progenitors to specify disproportionately the sizes and positioning of the primary cortical areas and that higher levels of EMX2 preferentially impart caudal-medial area identities, such as those associated with V1.

EMX2 and Cortical Size

Emx2 null mice have a cortical hemisphere that is 70% of wt size at P0, a reduction that is evident as early as E12.5 (Bishop et al., 2003). However, *Emx2* mutants do not have decreased proliferation rates or increased progenitor cell death during cortical neurogenesis (Shinozaki et al., 2002; Bishop et al., 2003), suggesting that the reduced size is due at least in part to a defect in an earlier patterning event that allocates early telencephalic progenitors to specific fates (Muzio et al., 2002a). *Emx2* overexpression in vitro increases cortical clone size (Heins et al., 2001). Although these findings suggest a relationship between EMX2 and cortical size and cell number, we find no difference in cortical surface area or laminar appearance and thickness between postnatal wt, *ne-Emx2* mice, and *Emx2*$^{+/-}$ mice.

EMX2 Influences on TCA Projections Are Limited to Their Area-Specific Patterning

The *Emx2* transgene is expressed in progenitors throughout the CNS, but its effect is limited. For example, dTh patterning is normal in *ne-Emx2* transgenics, even though dTh progenitors ectopically express *Emx2*. In *Emx2* nulls, TCAs exhibit subcortical pathfinding errors (Lopez-Bendito et al., 2002; Bishop et al., 2003), but TCA pathfinding is normal in *ne-Emx2* mice, further suggesting that dTh and subcortical structures that are involved in TCA guidance develop normally in *ne-Emx2* mice.

Our findings indicate that EMX2 not only confers area identity to cells that form the cortical plate but also specifies the expression of guidance molecules that control area-specific targeting of TCAs that are presumed to act in the subplate (Ghosh et al., 1990). Leingartner et al. (2003) have also shown that TCAs from dLG, which normally target V1, aberrantly invade S1 coincident with high levels of deep layer *Emx2*-AdV infection, indicating that higher levels of EMX2 specify cortical cells to have TCA guidance properties normally associated with V1. Shifts in area-specific TCA projections in *Emx2* mutants are consistent with this interpretation (Bishop et al., 2000; Mallamaci et al., 2000a) but are subject to the caveat that TCAs from dLG have aberrant subcortical pathfinding in *Emx2* nulls (but not *Emx2*$^{+/-}$ mice) (Lopez-Bendito et al., 2002). Inconsistent with our findings is the report that TCAs have a normal areal projection to cortex of neonatal *Fgf8* hypomorphic mice that have higher levels of graded *Emx2* (Garel et al., 2003). Large ablations of neocortex in the marsupial *Monodelphis domestica*, before TCAs arrive, result in a compression of area-specific TCA projections (Huffman et al., 1999), but whether genetic respecification is involved is not known.

Roles for EMX2 and FGF8 in Cortical Patterning

The graded expression of *Emx2* and likely other TFs in the cortical VZ is established by patterning centers that secrete signaling molecules, including FGFs expressed in the commissural plate at the rostral midline of the nascent neocortex (Shimamura and Rubenstein, 1997) (Figure 9A) that repress *Emx2* (Crossley et al., 2001) (Figure 9B) and BMPs and WNTs expressed in the cortical hem along the caudodorsal midline (Furuta et al., 1997; Grove et al., 1998) that positively regulate *Emx2* expression (Ohkubo et al., 2002; Theil et al., 2002). Electroporation in mice to overexpress *Fgf8* or diminish endogenous FGF8 results in repressed or enhanced expression of *Emx2* in the rostral VZ and S1 shifting caudally or rostrally, respectively (Fukuchi-Shimogori and Grove, 2001, 2003). Similarly, *Fgf8* hypomorphic mice have a higher level of graded *Emx2* expression in the cortical VZ (Garel et al., 2003). Thus, the S1 shifts

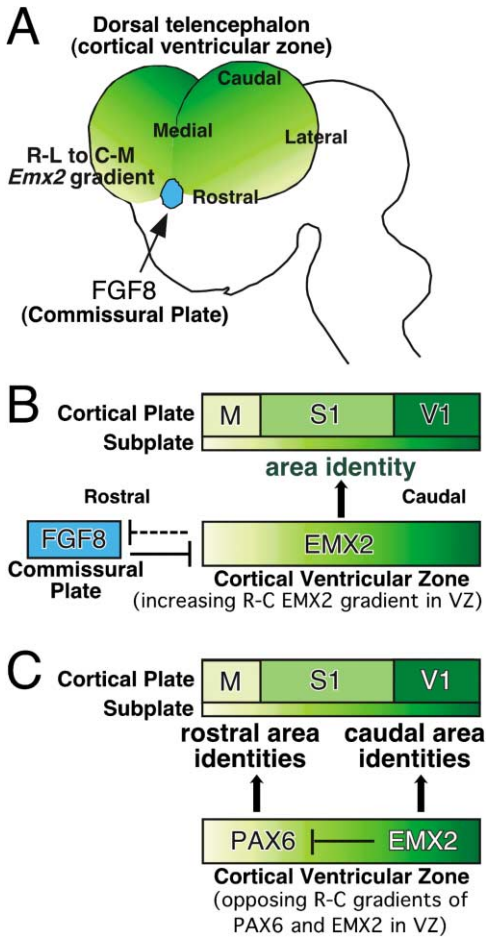

Figure 9. EMX2 Regulation of Patterning of Neocortex into Primary Areas

(A) The low rostral-lateral (R-L) to high caudal-medial (C-M) graded expression of *Emx2* in progenitors across the cortical ventricular zone (VZ) of dTel is established by signaling molecules, such as FGF8 secreted from the commissural plate, a midline domain positioned at the rostral margin of dTel. (B) FGF8 helps establish the graded expression of *Emx2* through repression before cortical neurogenesis begins. EMX2 appears to repress *Fgf8* expression and restrict its expression domain. Our findings show that the graded distribution of EMX2 in progenitors in the VZ directly participates in the specification of their positional, or area, identity, inherited by their neuronal progeny, which form the subplate and cortical plate. This EMX2 specification regulates axon guidance information in the subplate to establish area-specific TCA projections and determines the sizes and positioning of the primary cortical areas (also see Figures 1A and 8A). (C) EMX2 likely cooperates with other TFs, such as PAX6, to specify area identity. EMX2 represses *Pax6* expression, diminishing the influence of PAX6 in imparting rostral area identities and thereby contributing to the reduced sizes and rostral shifts of the rostrally located areas motor and S1 that are observed in *ne-Emx2* mice. See the Discussion for details. L, lateral; M, motor areas; R, rostral; S1, primary somatosensory area; V1, primary visual area.

are consistent with a model in which FGF8 regulates the level of graded *Emx2* expression in cortical progenitors, and EMX2 specifies the shift of S1 directly and/or by repressing *Pax6*.

However, Fukuchi-Shimogori and Grove (2003) conclude that EMX2 does not directly control arealization but solely acts indirectly by repressing *Fgf8* expression in the commissural plate. They report that ectopic expression of *Emx2* in the *Fgf8* domain in the commissural plate by electroporation in E10.5 cortical explants results in a dramatic downregulation of *Fgf8* and a later rostral shift in S1 in mice similarly electroporated in utero at E10.5. The shifts that we observe in S1 in homozygous *ne-Emx2* mice match the description of cases with rostral electroporation of *Emx2* in wt mice that result in a virtually complete loss of *Fgf8* expression in the commissural plate. Therefore, for the arealization changes in *ne-Emx2* mice to be solely mediated by the *Emx2* transgene repressing *Fgf8* expression would require that the *Fgf8* expression domain in the commissural plate be substantially reduced. However, this *Fgf8* domain in *ne-Emx2* mice is indistinguishable from wt at embryonic ages during and after FGF8 exerts its patterning influence.

Therefore, our data demonstrate that changes in arealization in *ne-Emx2* mice are not due to repression of *Fgf8* expression. Instead, the disproportionate changes in sizes of primary cortical areas and shifts in their positions in *ne-Emx2* mice must be due to the direct and combined effect of endogenous *Emx2* and the *Emx2* transgene in progenitors in the cortical VZ. This conclusion is supported by our findings that caudal primary areas V1 and A1 exhibit size changes and shifts in position in heterozygous *ne-Emx2* mice intermediate to wt and homozygous *ne-Emx2* mice, whereas rostral areas, such as S1, do not have significant changes; this selective effect on caudal areas is difficult to reconcile with a mechanism by which EMX2 acts solely by repressing *Fgf8* in the rostrally located commissural plate.

Complementary Actions of EMX2, PAX6, and Other Regulatory Proteins in Arealization

Diminishing endogenous FGF levels "rescues" shifts of gene markers in embryonic *Emx2* null mice (Fukuchi-Shimogori and Grove, 2003)—a finding that indicates the upregulation of other TFs that normally cooperate with EMX2 in arealization and compensate for its loss. For example, *Coup-TF1*, which is implicated in arealization (Zhou et al., 2001), is upregulated when FGF8 is diminished (Fukuchi-Shimogori and Grove, 2003; Garel et al., 2003).

Coup-TF1 (Liu et al., 2000) and *Lhx2* (Nakagawa et al., 1999) have caudal to rostral graded expression that parallels *Emx2* in the cortical VZ. We detect no change in their graded expression in embryonic *ne-Emx2* mice but find a flattening of the normally strongly graded, high rostral to low caudal expression of *Pax6*, consistent with an analysis of *Emx2* null mice suggesting that EMX2 represses *Pax6* (Muzio et al., 2002b). Marker analyses of embryonic *Pax6* mutant mice implicate PAX6 in areal patterning, particularly in imparting rostral area identities (Bishop et al., 2000, 2002). Thus, repression of *Pax6* in rostral VZ of *ne-Emx2* mice would diminish its influence in imparting rostral area identities and thereby contribute to the reduced sizes and shifts of rostral areas motor and S1 in *ne-Emx2* mice (Figure 9C).

Model of Areal Patterning of the Neocortex

The "combinatorial code model" of neuronal specification defined in the developing ventral spinal cord has become the dominant mechanism for specification of

neuronal identities (Jessell, 2000). In the spinal cord VZ, sonic hedgehog that is secreted by notocord and floorplate represses or induces expression of different TFs in graded patterns that constrict into sharply bordered patterns through mutual repression. This mechanism results in genetically distinct domains of progenitors, which generate different types of interneurons and motor neurons that are definable by their expression of unique subsets of TFs and other proteins.

We suggest that the mechanism that operates in cortex to specify area identities has similarities to but also important differences from the combinatorial code model. As in spinal cord, in cortex the initial graded expression of TFs, for example, *Emx2* and *Pax6*, in progenitors across the cortical VZ is established by signaling molecules secreted from patterning centers, and the graded expression of TFs across the cortical VZ is refined by crossrepression (present study; Muzio et al., 2002a). Later in the cortical plate, the expression of many genes, including *RORβ* (Nakagawa and O'Leary, 2003), *Coup-TF1* (Liu et al., 2000), and *Id2* (Rubenstein et al., 1999), develop disjunctive patterns that align with area borders. This patterned gene expression may develop by a progressive translation of the graded expression of *Emx2* through concentration-dependent differences in binding efficacy to promoter and repressor elements or its participation in the combinatorial action of multiple activators and repressors of transcription (O'Leary and Nakagawa, 2002). However, at no time during corticogenesis are sharply bordered patterns of TFs evident in the neocortical VZ, and all retain graded expression across the entire neocortical VZ.

Thus, in contrast to the spinal cord VZ, the neocortical VZ does not become parcellated into genetically distinct domains of progenitors. We propose that absolute levels of EMX2 in cortical progenitors specify the area identity of their progeny. In this model, increasing or reducing EMX2 in cortical progenitors results in a complete change in the area identity of their neuronal progeny, for example, from a V1 to an S1 identity, or an S1 to a V1 identity, respectively, rather than generating neurons exhibiting a mix of phenotypes characteristic of multiple areas or an aberrant phenotype. Further studies will be required to test and refine this proposed "cooperative concentration" model of cortical area patterning and determine the TFs that cooperate with EMX2 in this process.

Experimental Procedures

Mice

Morning of the vaginal plug is E0.5; embryos were also staged (Kaufman, 1994). The first 24 hr after birth is P0. Analyses were done blind to genotype. Animal care was in accordance with institutional guidelines.

Emx2$^{+/-}$ and *Emx2*$^{+/+}$ littermates were generated from heterozygous breeding pairs maintained on a C57/BL6 background (obtained from P. Gruss) and genotyped (Pelligrini et al., 1996).

To generate *ne-Emx2* transgenic mice, a 0.8 kb rat *Emx2* cDNA fragment was amplified by PCR and flanked with XhoI sites, using a cDNA clone as a template and sense (5′-GGTGGGCTCGAGGCTC GGCGCAGCATGTTTCA-3′) and antisense primers (5′-GCTAGACT CGAGGTGGGAATAGGTTTGTACT-3′) (XhoI sites are underlined; the ATG start codon of the open reading frame (ORF) of *Emx2* is double underlined. The PCR product contains the entire rat *Emx2* ORF, which is 100% identical in sequence to mouse *Emx2* (Leingartner et al., 2003), plus 12 bp upstream and 20 bp downstream. The PCR product was verified and cloned into the SalI site of the expression vector NesP/3introns (Zimmerman et al., 1994) (provided by U. Lendahl), placing the *Emx2* ORF downstream of 5.8 kb of rat *nestin* promoter sequence and upstream of a SV40 polyA signal, trailed by a 5.4 kb *nestin* genomic sequence, that provides enhancer activity. The *ne-Emx2* expression cassette (*nestin promoter/Emx2/polyA/nestin enhancer*) was purified and injected into the pronucleus of fertilized (C57BL/6 × BALB/c) F1 mouse oocytes (Hogan et al., 1994). Mice were genotyped by PCR using genomic DNA from the tail of postnatal and late embryonic stages or yolk sac from earlier embryos, a nestin-specific sense primer (5′-TCAACCCCTAAAAGC TCC-3′), and an *Emx2*-specific antisense primer (5′-GGACGGAGA GAAGGCGGT-3′), resulting in a transgene-specific band of 587 bp.

RT-PCR Detection of Transgene Expression

To detect specifically *ne-Emx2* transgene mRNA, RT-PCR was done on total RNA as described (Leingartner et al., 1994). Reverse transcription (RT) was primed with an *Emx2*-specific antisense oligo (5′-TGATTCTTCTCGAACGCG-3′), and PCR was performed with the same oligo and a *nestin*-specific sense primer (5′-TCAACCCC-3′). RT-PCR reaction was followed by a second round of PCR with nested primers for nestin (5′-TCAACCCCTAAAAGCTCC-3′) and *Emx2* (5′-GGACGGAGAG-3′ or 5′-AATCCGCTTCGGCTTTCG-3′), using 1/10^4 volume of the first reaction as template. Enzymes and buffers were from Qiagen. To rule out false positives, half of the DNase-treated sample was processed identically, except RT was omitted.

Northern Blot

Northern blot analysis was performed as described (Leingartner et al., 1994). Relative levels of *Emx2* expression were quantified using densitometry of digitized blot images (NIH image). Mean density was determined for each band, from which background was subtracted. The values presented are means from three or more blots.

In Situ Hybridization

^{35}S-labeled or digoxigenin (DIG)-labeled riboprobes that were used are as follows: *Emx2* (Leingartner et al., 2003), *Fgf8* (The Salk Institute), *cad8*, *Lhx2*, *Lhx9* (Nakagawa et al., 1999), *Pax6* (mouse full-length clone; O'Leary lab), *Gbx2* (mouse full-length clone; G. Chapman, University of Adelaide, Australia), and *COUP-TF1* (mouse clone; M.-J. Tsai, Baylor). In situ hybridization on 20–40 μm cryostat sections was performed as described (DIG, Nakagawa et al., 1999; ^{35}S, Liu et al., 2000). DIG whole-mount in situ hybridization was performed as described (Nakagawa et al., 1999). Relative gradients of *Emx2* and *Pax6* expression were quantified from sagittal sections of E10.5 wt and *ne-Emx2* mice (n = 4 for each mouse line and gene) (Figures 7G and 7H). Silver grains were counted in fields of 1.0 × 10^4 μm^2 at the rostral end, caudal end, and midpoint in the VZ of dTel. Data are expressed as the ratio of counts in each field to the total count in three fields in the same section.

Tangential Sections, Immunostaining, CO Histochemistry, Statistical Analysis, and DiI Tracing

Mice were perfused with cold 4% buffered paraformaldehyde; the cortical hemisphere was dissected free and postfixed between slide glasses and then cryoprotected. Tangential sections were cut at 40 μm. For immunostaining, sections were blocked, incubated with anti-serotonin (1:50,000; Immunostar) or anti-nestin (1:1,000; BD Biosciences Pharmingen) antibodies, detected with biotinylated secondary antibodies using Elite ABC kit (Vector). CO histochemistry was performed (Wong-Riley, 1979). Images of CO or serotonin-stained tangential sections were taken with a digital camera. Areas, lengths, and defined points were determined using Scion Image (Scion Corp) or Photoshop (Adobe). Excel (Microsoft) was programmed to calculate the axial position of barrel C3 and A1. Statistical analysis was done in SPSS (SPSS Inc.). DiI tracing of TCAs was done as described (Braisted et al., 1999).

Acknowledgments

Supported by NIH R37 NS31558 (D.D.M.O.) and a fellowship to T.H. from the Japan Society for the Promotion of Science. We thank U. Lendhal for the nestin promoter construct; P. Gruss for *Emx2*

knockout mice; Y. Nakagawa for help with diencephalic analyses; K. Yee and S.-J. Chou for advice; and T. McLaughlin for comments.

Received: December 22, 2003
Revised: April 23, 2004
Accepted: June 16, 2004
Published: August 4, 2004

References

Bishop, K.M., Goudreau, G., and O'Leary, D.D.M. (2000). Regulation of area identity in the mammalian neocortex by Emx2 and Pax6. Science *288*, 344–349.

Bishop, K.M., Rubenstein, J.L.R., and O'Leary, D.D.M. (2002). Distinct actions of Emx1, Emx2, and Pax6 in regulating the specification of areas in the developing neocortex. J. Neurosci. *22*, 7627–7638.

Bishop, K.M., Garel, S., Nakagawa, Y., Rubenstein, J.L.R., and O'Leary, D.D.M. (2003). Emx1 and Emx2 cooperate to regulate cortical size, lamination, neuronal differentiation, development of cortical efferents, and thalamocortical pathfinding. J. Comp. Neurol. *457*, 345–360.

Braisted, J.E., Tuttle, R., and O'Leary, D.D.M. (1999). Thalamocortical axons are influenced by chemorepellent and chemoattractant activities localized to decision points along their path. Dev. Biol. *208*, 430–440.

Crossley, P.H., Martinez, S., Ohkubo, Y., and Rubenstein, J.L.R. (2001). Coordinate expression of Fgf8, Otx2, Bmp4, and Shh in the rostral prosencephalon during development of the telencephalic and optic vesicles. Neuroscience *108*, 183–206.

Dahlstrand, J., Lardelli, M., and Lendahl, U. (1995). Nestin mRNA expression correlates with the central nervous system progenitor cell state in many, but not all, regions of developing central nervous system. Brain Res. Dev. Brain Res. *84*, 109–129.

Fujimiya, M., Kimura, H., and Maeda, T. (1986). Postnatal development of serotonin nerve fibers in the somatosensory cortex of mice studied by immunohistochemistry. J. Comp. Neurol. *246*, 191–201.

Fukuchi-Shimogori, T., and Grove, E.A. (2001). Neocortex patterning by the secreted signaling molecule FGF8. Science *294*, 1071–1074.

Fukuchi-Shimogori, T., and Grove, E.A. (2003). Emx2 patterns the neocortex by regulating FGF positional signaling. Nat. Neurosci. *6*, 825–831.

Furuta, Y., Piston, D.W., and Hogan, B.L. (1997). Bone morphogenetic proteins (BMPs) as regulators of dorsal forebrain development. Development *124*, 2203–2212.

Garel, S., Yun, K., Grosschedl, R., and Rubenstein, J.L.R. (2002). The early topography of thalamocortical projections is shifted in *Ebf1* and *Dlx1/2* mutant mice. Development *129*, 5621–5634.

Garel, S., Huffman, K.J., and Rubenstein, J.L.R. (2003). Molecular regionalization of the neocortex is disrupted in Fgf8 hypomorphic mutants. Development *130*, 1903–1914.

Ghosh, A., Antonini, A., McConnell, S.K., and Shatz, C.J. (1990). Requirement for subplate neurons in the formation of thalamocortical connections. Nature *347*, 179–181.

Grove, E.A., Tole, S., Limon, J., Yip, L., and Ragsdale, C.W. (1998). The hem of the embryonic cerebral cortex is defined by the expression of multiple Wnt genes and is compromised in Gli3-deficient mice. Development *125*, 2315–2325.

Heins, N., Cremisi, F., Malatesta, P., Gangemi, R.M., Corte, G., Price, J., Goudreau, G., Gruss, P., and Gotz, M. (2001). Emx2 promotes symmetric cell divisions and a multipotential fate in precursors from the cerebral cortex. Mol. Cell. Neurosci. *18*, 485–502.

Hogan, B., Constantini, F., and Lacey, E. (1994). Production of transgenic mice. In Manipulating the Mouse Embryo: A Laboratory Manual, B. Hogan, F. Constantini, and E. Lacey, eds. (Cold Spring Harbor, NY: Cold Spring Harbor Laboratory Press), pp. 217–252.

Huffman, K.J., Molnar, Z., Van Dellen, A., Kahn, D.M., Blakemore, C., and Krubitzer, L. (1999). Formation of cortical fields on a reduced cortical sheet. J. Neurosci. *19*, 9939–9952.

Jessell, T.M. (2000). Neuronal specification in the spinal cord: inductive signals and transcriptional codes. Nat. Rev. Genet. *1*, 20–29.

Jones, L., Lopez-Bendito, G., Gruss, P., Stoykova, A., and Molnar, Z. (2002). Pax6 is required for the normal development of the forebrain axonal connections. Development *129*, 5041–5052.

Kaufman, M.H. (1994). The Atlas of Mouse Development, Second Printing (San Diego, CA: Academic Press).

Leingartner, A., Heisenberg, C.P., Kolbeck, R., Thoenen, H., and Lindholm, D. (1994). Brain-derived neurotrophic factor increases neurotrophin-3 expression in cerebellar granule neurons. J. Biol. Chem. *269*, 828–830.

Leingartner, A., Richards, L.J., Dyck, R.H., Akazawa, C., and O'Leary, D.D.M. (2003). Cloning and cortical expression of rat Emx2 and adenovirus-mediated overexpression to assess its regulation of area-specific targeting of thalamocortical axons. Cereb. Cortex *13*, 648–660.

Liu, Q., Dwyer, N.D., and O'Leary, D.D.M. (2000). Differential expression of COUP-TFI, CHL1, and two novel genes in developing neocortex identified by differential display PCR. J. Neuroscience *20*, 7682–7690.

Lopez-Bendito, G., Chan, C.H., Mallamaci, A., Parnavelas, J., and Molnar, Z. (2002). Role of Emx2 in the development of the reciprocal connectivity between cortex and thalamus. J. Comp. Neurol. *451*, 153–169.

Magdaleno, S., Keshvara, L., and Curran, T. (2002). Rescue of ataxia and preplate splitting by ectopic expression of Reelin in reeler mice. Neuron *33*, 573–586.

Mallamaci, A., Muzio, L., Chan, C.H., Parnavelas, J., and Boncinelli, E. (2000a). Area identity shifts in the early cerebral cortex of Emx2$^{-/-}$ mutant mice. Nat. Neurosci. *3*, 679–686.

Mallamaci, A., Mercurio, S., Muzio, L., Cecchi, C., Pardini, C.L., Gruss, P., and Boncinelli, E. (2000b). The lack of Emx2 causes impairment of Reelin signaling and defects of neuronal migration in the developing cerebral cortex. J. Neurosci. *20*, 1109–1118.

Monuki, S.E., Porter, F.D., and Walsh, C.A. (2001). Patterning of the dorsal telencephalon and cerebral cortex by a roof plate-Lhx2 pathway. Neuron *32*, 591–604.

Muzio, L., and Mallamaci, A. (2003). Emx1, emx2 and pax6 in specification, regionalization and arealization of the cerebral cortex. Cereb. Cortex *13*, 641–647.

Muzio, L., DiBenedetto, B., Stoykova, A., Boncinelli, E., Gruss, P., and Mallamaci, A. (2002a). Conversion of cerebral cortex into basal ganglia in Emx2$^{-/-}$ Pax6$^{Sey/Sey}$ double-mutant mice. Nat. Neurosci. *5*, 737–745.

Muzio, L., DiBenedetto, B., Stoykova, A., Boncinelli, E., Gruss, P., and Mallamaci, A. (2002b). Emx2 and Pax6 control regionalization of the pre-neuronogenic cortical primordium. Cereb. Cortex *12*, 129–139.

Nakagawa, Y., and O'Leary, D.D.M. (2001). Combinatorial expression patterns of LIM-homeodomain and other regulatory genes parcellate developing thalamus. J. Neurosci. *21*, 2711–2725.

Nakagawa, Y., and O'Leary, D.D.M. (2003). Dynamic patterned expression of orphan nuclear receptor genes RORα and RORβ in developing mouse forebrain. Dev. Neurosci. *25*, 234–244.

Nakagawa, Y., Johnson, J.E., and O'Leary, D.D.M. (1999). Graded and areal expression patterns of regulatory genes and cadherins in embryonic neocortex independent of thalamocortical input. J. Neurosci. *19*, 10877–10885.

Ohkubo, Y., Chiang, C., and Rubenstein, J.L.R. (2002). Coordinate regulation and synergistic actions of BMP4, SHH and FGF8 in the rostral prosencephalon regulate morphogenesis of the telencephalic and optic vesicles. Neuroscience *111*, 1–17.

O'Leary, D.D.M. (1989). Do cortical areas emerge from a protocortex? Trends Neurosci. *12*, 400–406.

O'Leary, D.D.M., and Nakagawa, Y. (2002). Patterning centers, regulatory genes and extrinsic mechanisms controlling arealization of the neocortex. Curr. Opin. Neurobiol. *12*, 14–25.

O'Leary, D.D.M., Schlaggar, B.L., and Tuttle, R. (1994). Specification

of neocortical areas and thalamocortical connections. Annu. Rev. Neurosci. *17*, 419–439.

Pelligrini, M., Mansouri, A., Simeone, A., Boncinelli, E., and Gruss, P. (1996). Dentate gyrus formation requires *Emx2*. Development *122*, 3893–3898.

Rakic, P. (1988). Specification of cerebral cortical areas. Science *241*, 170–176.

Ringstedt, T., Linnarsson, S., Wagner, J., Lendahl, U., Kokaia, Z., Arenas, E., Ernfors, P., and Ibanez, C.F. (1998). BDNF regulates reelin expression and Cajal-Retzius cell development in the cerebral cortex. Neuron *21*, 305–315.

Rubenstein, J.L., Anderson, S., Shi, L., Miyashita-Lin, E., Bulfone, A., and Hevner, R. (1999). Genetic control of cortical regionalization and connectivity. Cereb. Cortex *9*, 524–532.

Shimamura, K., and Rubenstein, J.L.R. (1997). Inductive interactions direct early regionalization of the mouse forebrain. Development *124*, 2709–2718.

Shinozaki, K., Miyagi, T., Yoshida, M., Miyata, T., Ogawa, M., Aizawa, S., and Suda, Y. (2002). Absence of Cajal-Retzius cells and subplate neurons associated with defects of tangential cell migration from ganglionic eminence in Emx1/2 double mutant cerebral cortex. Development *129*, 3479–3492.

Simeone, A., Acampora, D., Gulisano, M., Stornaiuolo, A., and Boncinelli, E. (1992a). Nested expression domains of four homeobox genes in developing rostral brain. Nature *358*, 687–690.

Simeone, A., Gulisano, M., Acampora, D., Stornaiuolo, A., Rambaldi, M., and Boncinelli, E. (1992b). Two vertebrate homeobox genes related to the Drosophila empty spiracles gene are expressed in the embryonic cerebral cortex. EMBO J. *11*, 2541–2550.

Suzuki, S.C., Inoue, T., Kimura, Y., Tanaka, T., and Takeichi, M. (1997). Neuronal circuits are subdivided by differential expression of type-II classic cadherins in postnatal mouse brains. Mol. Cell. Neurosci. *9*, 433–447.

Theil, T., Aydin, S., Koch, S., Grotewold, L., and Ruther, U. (2002). Wnt and Bmp signalling cooperatively regulate graded Emx2 expression in the dorsal telencephalon. Development *129*, 3045–3054.

Wong-Riley, M. (1979). Changes in the visual system of monocularly sutured or enucleated cats demonstrable with cytochrome oxidase histochemistry. Brain Res. *171*, 11–28.

Wong-Riley, M.T., and Welt, C. (1980). Histochemical changes in cytochrome oxidase of cortical barrels after vibrissal removal in neonatal and adult mice. Proc. Natl. Acad. Sci. USA *77*, 2333–2337.

Zhou, C., Tsai, S.Y., and Tsai, M.J. (2001). COUP-TFI: an intrinsic factor for early regionalization of the neocortex. Genes Dev. *15*, 2054–2059.

Zimmerman, L., Parr, B., Lendahl, U., Cunningham, M., McKay, R., Gavin, B., Mann, J., Vassileva, G., and McMahon, A. (1994). Independent regulatory elements in the nestin gene direct transgene expression to neural stem cells or muscle precursors. Neuron *12*, 11–24.